Frequency Chirp Stabilization in Semiconductor Distributed Feedback Lasers With External Control

F. Grillot[1,2], J. G. Provost[3], K. Kechaou[2], B. Thedrez[2] and D. Erasme[2]

[1] *Université Européenne de Bretagne, INSA, CNRS FOTON, 20 av. des Buttes de Coësmes, 35043 Rennes, France*

[2] *Telecom Paristech, Ecole Nationale Supérieure des Télécommunications, CNRS LTCI, 46 rue Barrault, 75634 Paris Cedex, France*

[3] *III-V Lab, a joint lab of 'Alcatel-Lucent Bell Labs France', 'Thales Research and Technology' and 'CEA Leti', Route de Nozay, 91460 Marcoussis, France*

frederic.grillot@telecom-paristech.fr

ABSTRACT

It is well known that current modulation in diode lasers generates amplitude (AM) and optical frequency (FM) modulations. The frequency chirp under direct current modulation originates from variations in the carrier density and from the finite difference in carrier density between the laser on and off states. Modulation of the carrier density modulates the gain and the optical index causing the resonant mode to shift. This frequency chirp broadens the spectrum, which is a serious limitation for high-speed applications and optical fiber communications. At low frequencies, thermal effects also alter the frequency chirp. The aim of this paper is to show that the laser's frequency chirp can be modified using an external control technique. The chirp response is evaluated via the determination of the chirp-to-power ratio (CPR) through a Mach-Zehnder interferometer. Experiments demonstrate that when an external optical feedback is properly adjusted, the CPR can be severely decreased over a wide range of modulation frequencies as compared to the free-running case. These preliminary results obtained on quantum well distributed feedback lasers (QW DFB) with low normalized coupling coefficient (κL) demonstrate how to stabilize the CPR through the DFB facet phase effects or parameters such as the linewidth enhancement factor. In order to confirm this frequency chirp engineering, self-consistent calculations based on the transfer matrix method are also presented.

I. INTRODUCTION

In 1.55-µm DFB lasers, the frequency chirp is the main limitation of high bit rate systems due to the dispersion in standard optical fibers. For high-speed applications, this frequency chirp is known to broaden the modulated spectrum, which is a serious limitation in optical fiber communications [1]. One way to look at the frequency chirp is to investigate the CPR, which takes into account the index changes, created by both the modulation of the carrier density and thermal effects. As a result, the total CPR≡ΔF/ΔP (with ΔF the amplitude of the FM and ΔP the variation in the optical power) can be written as the sum of two major contributions [2]:

$$\frac{\Delta F}{\Delta P}=\left(\frac{\Delta F}{\Delta P}\right)_{carrier}+\left(\frac{\Delta F}{\Delta P}\right)_{thermal} \tag{1}$$

where,

$$\left(\frac{\Delta F}{\Delta P}\right)_{thermal}=\frac{\left(1-\eta_{wp}\right)V_{th}Z_T\dfrac{d\nu}{dT}}{\eta\left(1+j\omega\tau_T\right)} \tag{2}$$

$$\left(\frac{\Delta F}{\Delta P}\right)_{carrier}=\frac{\alpha_H}{4\pi}\frac{\eta_i}{qV_p\eta}\frac{\varepsilon_P}{1+\varepsilon_P P}\left(1+j\frac{\omega}{\gamma_{PP}}\right)H(j\omega) \tag{3}$$

with,

$$\gamma_{PP} = \Gamma_C v_g a_p S \tag{4}$$

and,

$$H(j\omega) = \frac{\omega_r^2}{\omega_r^2 - \omega^2 + j\omega\gamma} \tag{5}$$

In equation (2), $\omega/2\pi$ is the electrical frequency of modulation, η_{wp} is the wall-plug efficiency of the output power P_{out}/P_{in}, Z_T is the thermal impedance of the laser structure, V_{th} is the threshold voltage of the laser which is assumed roughly constant above threshold, τ_T is the thermal time constant typically in the range of a few microseconds and yielding to thermal cutoff frequencies in the few hundred kilohertz range. The last coefficient $d\upsilon/dT$ represents the cavity mode shift with temperature which is typically of about 10 GHz/K. In equation (3), (4) and (5), S is the photon density, α_H is the so-called linewidth enhancement factor, η and η_i are the external and internal quantum efficiencies respectively, q is the elementary charge of the electron, ε_P is the gain compression factor, $\omega_r/2\pi$ is the electron-photon relaxation frequency, γ is the damping factor, Γ_C is the optical confinement factor, v_g is the group velocity, V_p is the photon volume in the active region and a_p is a constant taking into account the gain reduction at high photon densities.
This paper aims to demonstrate that the frequency chirp and so the CPR can be stabilized with a proper controlled external optical feedback over a wide range of modulation frequencies. It is well-known that the performance of a semiconductor laser can be strongly altered by any type of external optical feedback [3]. During early stages of research, the importance of the distance between the laser facet and the external mirror reflector was pointed out in determining the nature of the semiconductor laser's response to optical feedback. In fact, optical feedback effects in DFB lasers is a predominant effect mostly when the Bragg grating reflectivity is low (i.e low κL) in such a way that the DFB laser becomes very sensitive to the facets reflectivities. Therefore, small reflections in the percent range which originate from fiber facets or any other optical elements introduced into the light path can dramatically affect the laser stability [4][5][6]. Although external optical feedback can be considered as a source of instability in some situations, it also has several beneficial effects that can improve the laser performance. It can be used to reduce the linewidth of the emitted light or in other applications such as encryption based on chaos, for frequency tuning or velocity measurements [4][5]. The paper shows frequency chirp control obtained on QW DFB lasers operating under proper feedback conditions. It is demonstrated that the CPR remains constant over a wide range of modulation frequencies, which is of first importance for future optical telecommunication systems. Under the best feedback conditions the CPR does not exceed 106 MHz/mW on average from 10 kHz to 10 GHz, which corresponds to a reduction by a factor of 6.3 as compared to the solitary case. In order to confirm the frequency chirp stabilization, self-consistent calculations based on the transfer matrix method are presented and found in good agreement with the experiments. Numerical simulations also point out that the laser's feedback sensitivity is strongly dependent on the (κL) value, which controls the amplitude of the spatial hole burning (SHB).

II. EXPERIMENTAL RESULTS

The QW DFB laser under study is a buried ridge stripe (BRS) structure with a high reflection (HR) coating on the rear facet and an antireflection (AR) coating on the front facet in order to allow for high efficiency. The device is 350 μm long with an active layer made of six InGaAsP QWs. The grating defined in a quaternary layer localized over the active region was measured to be about 30 cm^{-1} (κL~0.8). In a similar way as for conventional DFB lasers, a standard holographic process is used to fabricate a single pitch grating over the full wafer [7]. The threshold current value is I_{th}=8 mA with an external efficiency η=0.26 W/A at 25°C. The objective of the experiment is to determine the characteristics of the FM contribution induced by the current modulation under optical feedback conditions. The CPR as well as the linewidth enhancement factor is also measured. As shown in figure 1, the implementation of the optical feedback loop is based on a 4-port optical coupler. Emitted light is injected into port 1 using a lensed fiber. The optical feedback is created with a high-reflectivity coated fiber in port 3. Its level is controlled via a variable optical attenuator (VOA) and its value is determined by measuring the power in port 2. Port 4 is then directly connected to a Mach-Zehnder (MZ) interferometer for chirp characterizations [8]. A polarization controller (PC) is used to make the feedback beam's polarization identical to that of the emitted wave in order to maximize the feedback effects. The quantity of injected

feedback into the laser is defined as the ratio $\Gamma = P_1/P_0$ where P_1 is the power returned to the facet and P_0 the emitted one. The feedback experiment is studied under the long external cavity condition [9] that assumes that $\omega_r\tau >> 1$ where τ is the external round trip time in the order of several hundred nanoseconds. Measurements are made for a pump current of $2.4\times I_{th}$, which corresponds to an emitting power of $P_0 \approx 3$ mW. Coupling loss coefficient between the laser output and the optical fiber was kept constant to about 3 dB during the whole experiments.

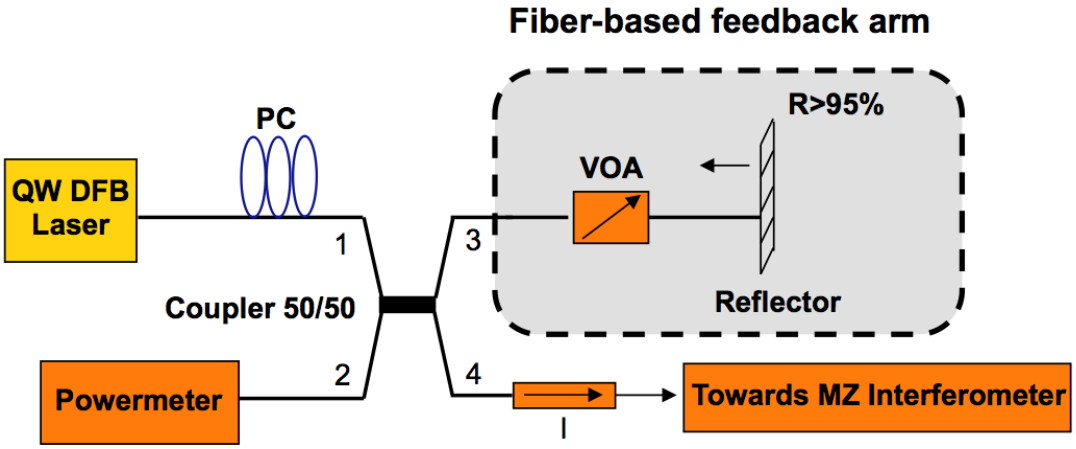

Fig. 1. Schematic of the optical feedback loop

Figure 2 shows the amplitude (blue) and the phase (red) of the CPR as a function of the frequency modulation for the solitary QW DFB laser emitting at 1550 nm. At low frequencies ($\omega/2\pi < 10$ MHz), thermal effects are predominant. For instance, at 30 kHz, the amplitude and the phase of the CPR are ~1.0 GHz/mW and ~140° respectively. When 10 MHz < $\omega/2\pi$ < 1 GHz, AM and FM modulations are in-phase (adiabatic regime) and the amplitude of the CPR reaches 650 MHz/mW at $\omega/2\pi$=500 MHz. In that case, thermal effects are no longer significant compare to electrical effects created by the modulation of the carrier density. Then, when $\omega/2\pi$>1GHz, relaxation oscillations between the carrier and photon numbers lead to a transient chirp with larger CPR values of about 1.5 GHz/mW at 10 GHz and a phase difference approaching 90°.

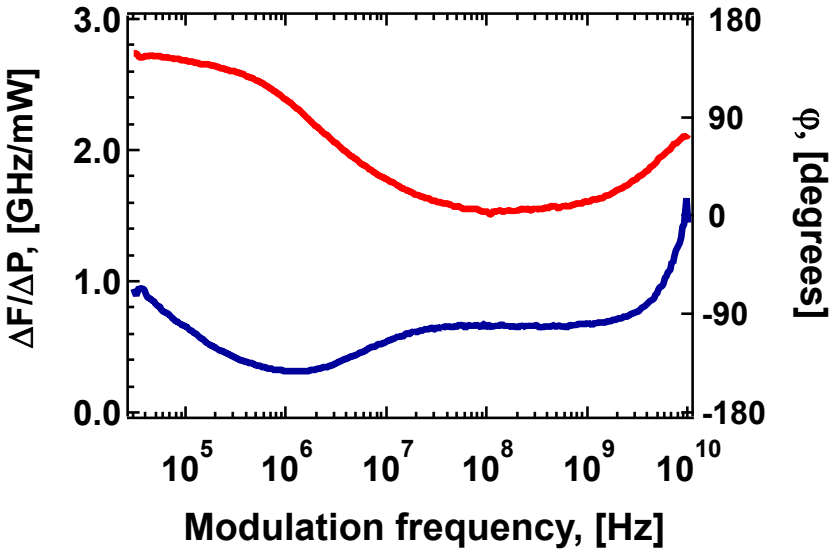

Fig. 2. Amplitude (blue) and phase (red) of the CPR as a function of the modulation frequency for the solitary QW DFB laser.

Figures 3 show both the amplitude and the phase of the CPR for various feedback levels (a) Γ=1.4×10^{-6}, (b) Γ=1.5×10^{-5}, (c) Γ=1.6×10^{-4}, and (d) Γ=5.5×10^{-3}. The results demonstrate that the use of a controlled optical feedback can modify both the thermal and adiabatic chirps. It is shown that the adiabatic CPR measured at $\omega/2\pi$=500 MHz is significantly decreased from about 650 MHz/mW in the solitary case down to 65 MHz/mW at the highest feedback level. Under the best feedback conditions the CPR does not exceed 106 MHz/mW on average from 10 kHz to 10 GHz, which corresponds to a reduction by a factor of 6.3 as compared to the solitary case. In order to clearly illustrate the frequency chirp stabilization, figure 4 also shows the measured adiabatic CPR (squared markers) at $\omega/2\pi$=500 MHz as a function of the optical feedback strength. The solid line is used for guiding eyes only. As shown in figures 3, the optical feedback can also modify the transient chirp. For instance, for $\omega/2\pi$=10 GHz, the transient chirp can be improved by a factor of 2 as compared to the free-running case. However, the amplitude of the optical feedback has to be controlled carefully because figure 3 also shows the occurrence of some parasitic peaks that are related to external cavity modes (ECM). ECM pop-up when the modulation frequency gets close to the laser's relaxation frequency. One solution to clean the CPR would be to shorten the length of the external cavity. Decreasing the external cavity length reduces significantly the number of ECM involve in the laser's stability and then leads to a translation of the residual parasitic peaks to the higher frequency range.

The reduction of the CPR can be explained through different effects. One explanation can be related to the linewidth enhancement factor variations induced by optical feedback. Figure 5 shows the measured $2\beta/m$ (with $\beta \equiv \Delta F/f_m$ and $m \equiv \Delta P/P_0$, with $f_m=\omega/2\pi$) ratio as a function of the modulation frequency. The linewidth enhancement factor is extracted from this ratio through the so-called relationship [10],

$$\frac{2\beta}{m} = \alpha_H \sqrt{1+\left(\frac{\omega_c}{\omega_m}\right)^2} \tag{6}$$

In (6), ω_c is defined as the roll-off frequency typically in the range of hundreds of MHz to few GHz depending on the output power level. Thus, for high modulation frequencies such as $\omega_m >> \omega_c$, a condition which is easily reached in our experiments (the maximum modulation frequency is about 20 GHz range), the factor $2\beta/m$ directly equals to the laser's linewidth enhancement factor. For low modulation frequencies, the ratio $2\beta/m$ becomes inversely proportional to the modulation frequency. In figure 5, the measured $2\beta/m$ ratio is plotted starting from 50 MHz (beyond the thermal effects) for the solitary case (red plot) and for a feedback level of about Γ=1.5×10^{-5} (blue plot). As predicted by (6), the function $2\beta/m$ tends asymptotically to the linewidth enhancement factor, which is estimated to be about 3.2 in the absence of external perturbation. However, with optical feedback the measured linewidth enhancement factor decreases down to about 1.8. According to equation (3), decreasing such a parameter by a factor of about 2 can partially explain the variation of the adiabatic chirp.

Let us recall that the adiabatic chirp can also be modified by the DFB facet phases. The optical feedback is known to modify the facet phases related to the front facet reflectivity [11]. Such variations both in amplitude and in phase can cause the chirp to deviate from the free-running values as theoretically discussed in section III.

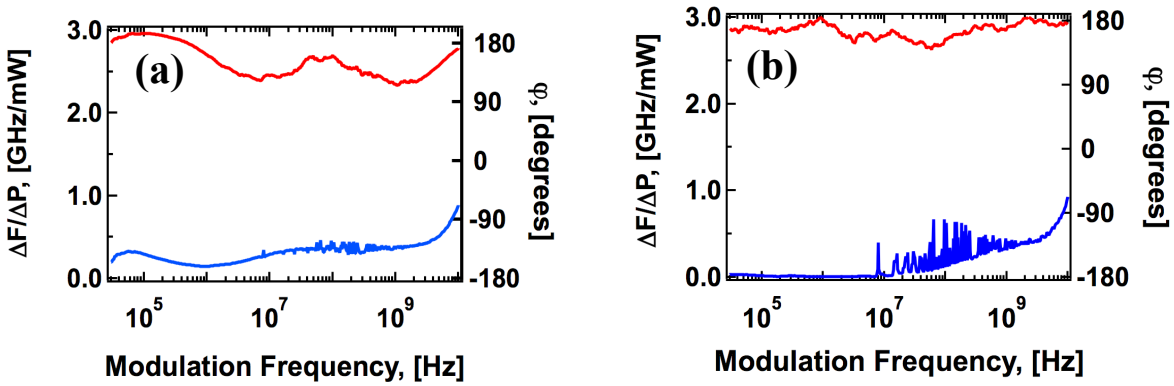

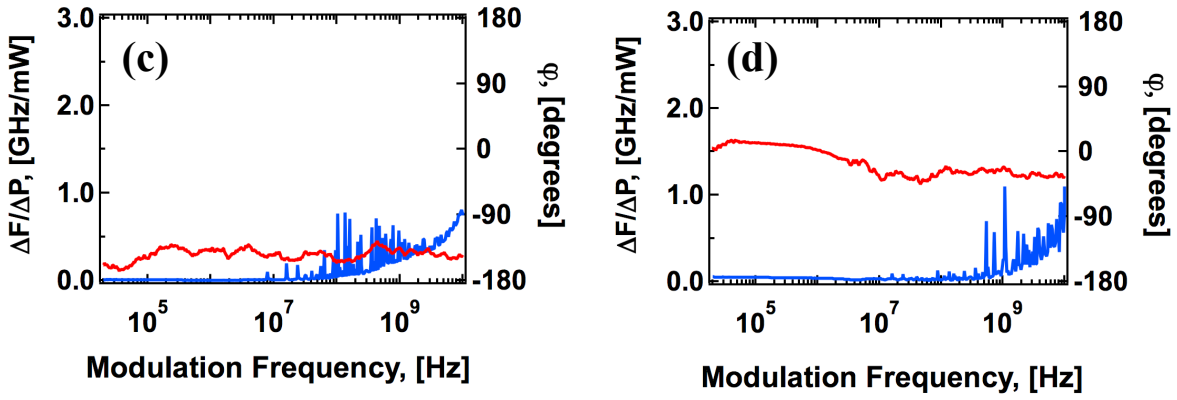

Fig. 3. Amplitude (blue) and phase (red) of the CPR as a function of the modulation frequency for various optical feedback Γ (a) Γ=1.4×10^{-6}, (b) Γ=1.5×10^{-5}, (c) Γ=1.6×10^{-4}, and (d) Γ=5.5×10^{-3}.

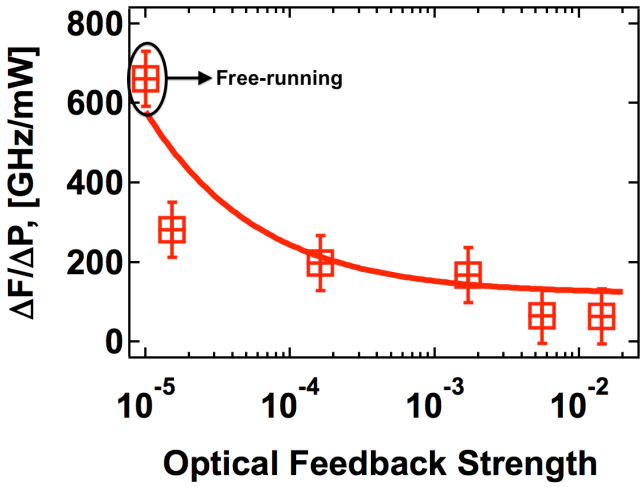

Fig. 4. Measured adiabatic CPR at 500 MHz as a function of the optical feedback strength for the QW DFB laser.

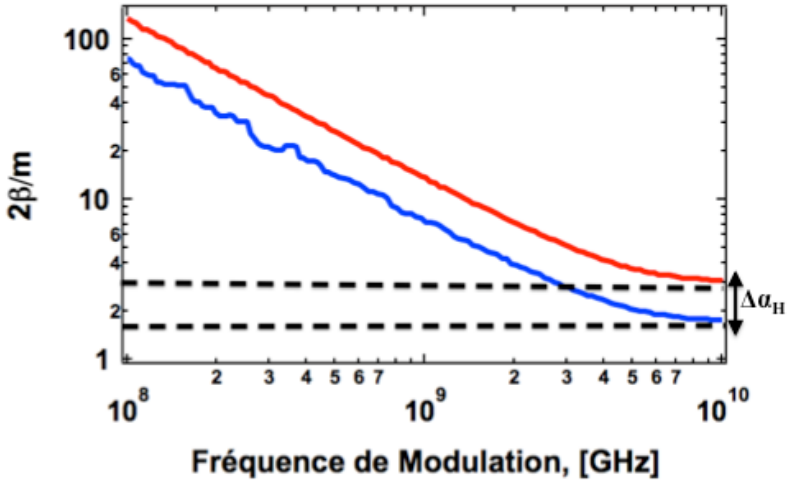

Fig. 5. Measured 2β/m ratio as a function of the modulation frequency for the solitary case (red plot) and for an optical feedback of about Γ=1.5×10^{-5} optical feedback (blue plot).

Figures 3 also show that the external control provokes a modification of the CPR's phase. This last point is of first importance because it shows that the delayed field can be properly used to control the phase of the CPR and the sign of the frequency chirp from negative (Fig. 3 (a) and (b)) to positive (Fig. 3 (c) and (d)). Indeed, it is known that the red chirp can be a source of penalty under transmissions across optical fibers while lasers with blue chirp are usually preferable for long-haul applications [12]. Finally, figures 3 demonstrate that the optical feedback efficiently cleans the thermal chirp. According to relationship (2) the thermal chirp can be curve-fitted based on a one pole analytic function such as:

$$\left(\frac{\Delta F}{\Delta P}\right)_{thermal} = \frac{A}{1 + j\omega\tau_T} \tag{7}$$

As an example, figure 6 shows the measured thermal chirp up to 200 kHz for the solitary laser and for a feedback case of I=1.5×10^{-5} (case (b)). The red solid line corresponds to the curve-fitting based on (7). From the curve-fitting coefficient A is found to significantly decrease from 0.93 GHz/mW in the free running case down to about 0.04 GHz/mW in presence of optical feedback. The cutoff frequency related to coefficient τ_T is also modified from about 9 μs to 22 μs.

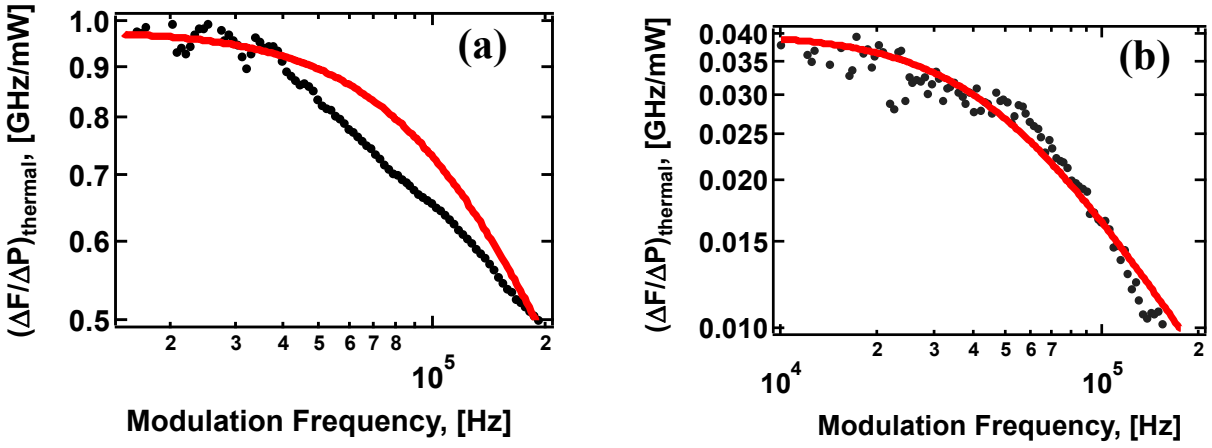

Fig. 6. Measured thermal chirp for the solitary case (a) and with optical feedback (b). The red solid lines correspond to the curve-fitting based on relationship (7).

Assuming that in typical DFB lasers, the thermal impedance Z_T is about 0.1 K/mW, dv/dT is 10 GHz/K and $(1-\eta_{sp})V_{th} \approx$ 1V, it appears that the use of a proper optical feedback decreases both the amplitude and the cutoff frequency of the thermal chirp. The change in the amplitude can be explained via the modification of the threshold voltage across the pn junction. The dependence of voltage changes on the feedback ratio is related to a reduction of the quasi-Fermi level related to the enhanced stimulated emission [13]. Modifications of the frequency shift or of the wall plug efficiency η_{wp} may be also possible but these assumptions needs more investigations and remains beyond the scope of the paper.

III. NUMERICAL MODELLING

We have performed numerical calculations based on the transfer matrix method (TMM) [14]. The aim is to calculate the QW DFB laser performance at threshold and to predict its static behaviour above-threshold. The method is applicable to any laser design. The DFB laser structure is divided into N sections consisting of many grating periods in which all physical parameters, like the injection current, the material gain the photon density, the carrier density and the refractive index are assumed to be homogeneous. The laser is modelled by assimilating the Bragg grating to a rectangular network.

The transfer matrix for one corrugation period is defined by:

$$\overline{M_{Period}} = \begin{bmatrix} \frac{n_1+n_2}{2n_1} & \frac{n_1-n_2}{2n_1} \\ \frac{n_1-n_2}{2n_1} & \frac{n_1+n_2}{2n_1} \end{bmatrix} \cdot \begin{bmatrix} e^{k_2 l} & 0 \\ 0 & e^{-k_2 l} \end{bmatrix} \cdot \begin{bmatrix} \frac{n_1+n_2}{2n_2} & \frac{n_2-n_1}{2n_2} \\ \frac{n_2-n_1}{2n_2} & \frac{n_1+n_2}{2n_2} \end{bmatrix} \cdot \begin{bmatrix} e^{k_1 l} & 0 \\ 0 & e^{-k_1 l} \end{bmatrix} \tag{8}$$

where n_1 and n_2 are the refractive indices, and k_1 and k_2 are the complex propagation constants in the two refractive index regions. The real part of the propagation constant is determined by the net gain, which is non-uniform along the device for the case of index-coupled DFB laser. The imaginary part depends on refractive index, which affects the frequency shift of the laser. The transfer matrix throughout the Bragg grating in sections is calculated from the m power of the transfer matrix for one corrugation period. To describe completely a DFB laser with cleaved facets, the transfer matrix can be written as:

$$\overline{M} = \overline{R_1} \cdot \overline{\phi_1} \cdot \left(\overline{M_{Period}}\right)^{m_N} \cdots\cdots \left(\overline{M_{Period}}\right)^{m_i} \cdots \left(\overline{M_{Period}}\right)^{m_2} \cdot \left(\overline{M_{Period}}\right)^{m_1} \overline{\phi_2} \cdot \overline{R_2} \tag{9}$$

where $\overline{R_1}$ and $\overline{R_2}$ are the reflectivity matrix at the left and right side, $\overline{\phi_1}$ and $\overline{\phi_2}$ are the partial propagation matrix corresponding to incomplete corrugation period at left and right facets and m_i is the number of period in the ith section. The gain versus carrier density N can be well approximated by a logarithmic formula including the gain compression effect in the vicinity of the emission frequency:

$$g(N,P) = \frac{g_0 \cdot \ln\left(\frac{e d_{qw} B_{rad} N^2}{J_0}\right)}{1+\varepsilon P} \tag{10}$$

In this approximation, g_0, e, d_{qw}, B_{rad}, J_0, ε, N and P are respectively the empirical gain coefficient, the electron charge, the thickness of one quantum well, the radiative recombination coefficient, the transparency current density, the gain compression coefficient, the carrier density and the photon density. At threshold, the net gain must offset the losses:

$$g = \alpha_{tot} = \alpha_{\text{int}} + 2\alpha_{DFB} \tag{11}$$

In equation (11) α_{DFB} represents the cavity loss and α_{int} is the internal losses which depend on the carrier density N including losses caused by the diffraction on technological inhomogeneities, light propagation and absorption losses in InP layers and differential losses in wells. For TMM, the oscillation condition at threshold is computed by using:

$$\overline{M}_{11}(\alpha,\lambda) = 0 \tag{12}$$

Assuming that n_1 and n_2 are uniform along the cavity, a prediction-correction method has been used to calculate the lasing mode represented by (α_{th},λ_{th}). In fact, the initial guesses (α_i , λ_i) of solutions correspond to Fabry-Perot modes. After calculating the value of $\overline{M}_{11}$ for (α_i , λ_i), (α_i+dα , λ_i) and, (α_i , λ_i+dλ), we compute the relative variations allowing the correction of the values of α and λ. This procedure is iteratively repeated until a relative variation less than 10^{-9} is reached. Above-threshold, the carrier distribution along the cavity shifts from uniform to non-uniform leading to intra-cavity Spatial Hole Burning (SHB). The resulting spatial index variation locally affects the grating, which becomes slightly non-uniform. This leads to cavity modes deviation consistent with the new distribution of the refractive index. The above-threshold resolution method was described in reference [15]. Indeed, for uniform-injected current, an iterative procedure is adopted. It consists on the resolution of the oscillation condition (12) using the new photon and carrier density distribution calculated from the previous solutions at lower injected current. The new obtained solution (α, λ) leads to another distribution of photon and carrier. Therefore, we re-solve (12). All steps are repeated until reaching an unchanged (α, λ).

When the laser is exposed to external feedback, the lasing frequency and the carrier density distribution deviates from

their original values. In the case of the QW DFB laser under study, the complex reflectivities can be expressed as follows [16]:

$$\tilde{r}_{AR,HR} = r_{AR,HR}\, e^{-i\varphi_{AR,HR}} \tag{13}$$

where $\varphi_{AR,HR}$ represents the facet phases terms depending on the position of the facets in the corrugation and $r_{AR,HR}$ the amplitude reflectivities on the front and on the back facets respectively. Under the weak optical feedback assumption, the equivalent amplitude AR facet reflectivity submitted to the delayed field can be written as [16]:

$$r_{AR,eq} = \tilde{r}_{AR} + \left(1 - \left|\tilde{r}_{AR}\right|^2\right) f_{ext}\, e^{-i\omega\tau} \tag{14}$$

with f_{ext} the optical feedback strength (f_{ext}<<1) and τ the external roundtrip time. In what follows the effects of the optical feedback on the adiabatic chirp are conducted for several AR front facet reflectivitites. Using the TMM, the simulated adiabatic chirp of the DFB laser under study is plotted in figure 7 as a function of the output power for various feedback conditions assuming 0%< $R_{AR,eq} = \left|r_{AR,eq}\right|^2$ <4%.

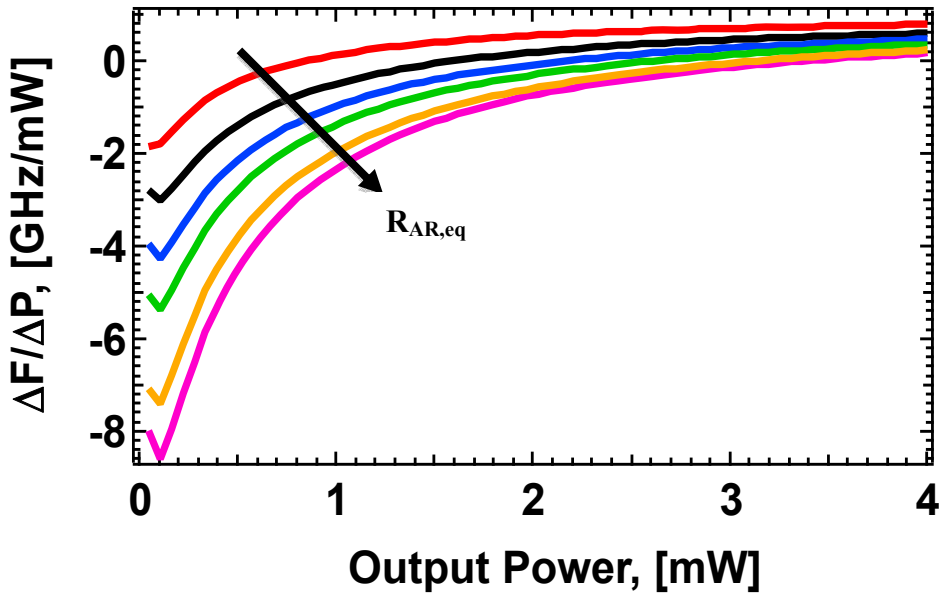

Fig. 7. Calculated adiabatic chirp as a function of the output power for various feedback conditions, κL= 0.8

At low output power, the chirp is strongly disturbed by the SHB effects. In fact, the optical field longitudinal distribution is not uniform and depends on facet phases. The heterogeneity of carrier density, which evolves with injected current, impacts the refractive index profile leading to wavelength shifts. Thus, depending on the feedback conditions, the repartition of the internal optical power is modified and varies along the longitudinal axis of the laser cavity. At high output power, the chirp converges independently of the feedback condition to a positive value, which is about 730 GHz/mW. This is due to the predominance of the gain compression effect against SHB.

Figure 8(a) shows a zoom from figure 7 between 3.1 and 3.5 mW output power. As experimentally observed, simulations confirm that the optical feedback can indeed stabilize the adiabatic chirp. In order to match our experimental conditions described in section II, figure 8(b) depicts the simulated values of the adiabatic chirp at P_0=3.36 mW (squared markers) as a function of the effective facet reflectivity which is related to the optical feedback strength

according to (14). The solid line is used for guiding eyes only. Thus, calculations are in a good agreement with the experimental values depicted in figure 4 since overall simulated variation is from 750 MHz/mW for R_{AR}=0% (solitary case) down to 65 MHz/mW with R_{AR}≈3%.

In order to investigate the relevant device parameters, figures 9 shows the calculated adiabatic chirp for κL=0.5 with L=350 μm. Front facet reflectivity is 0.1% (green plots), 1% (red plots) and 2% (blue plots) respectively. Compared to figure 7, decreasing (κL) leads to an increase of the laser's sensitivity to the optical feedback. This effect can be attributed to a lower intra-cavity photon density, which makes the laser more sensitive to external perturbations. Thus, optical reflections even in the percent range strongly enhance the SHB effects leading to a larger frequency chirp discrepancy especially at low output powers.

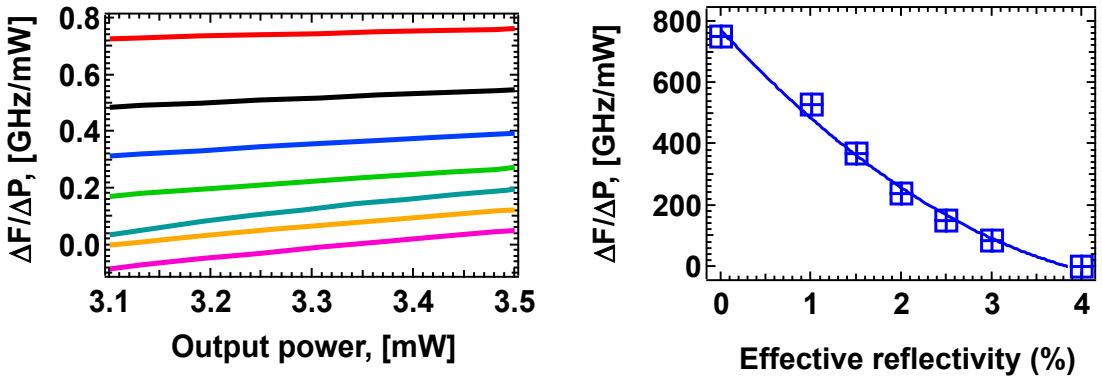

Fig. 8. (a) Zoom from figure 7 showing the calculated adiabatic chirp as a function of the output power for various feedback conditions (κL= 0.8) ; (b) Calculated adiabatic chirp as a function of the effective front facet reflectivity (κL= 0.8, P_0=3.5 mW).

For instance, figure 9 shows that when increasing the front facet reflectivity, the calculated adiabatic chirp at 1 mW drastically decreases from about 2 GHz/mW down to 45 MHz/mW. As previously mentioned at high output power, the chirp converges independently of the feedback condition to a positive value because of the predominance of the nonlinear gain effects. Figure 9 is of first importance because it also points out that if the optical feedback strength gets too large, the adiabatic chirp can turn from blue to red. As a result, the controlled optical feedback has to be properly adjusted to minimize or to zero the adiabatic chirp. This can be obtained by considering a tradeoff between a proper cavity design coupled to a controlled delayed field having the required properties both in amplitude and in phase.

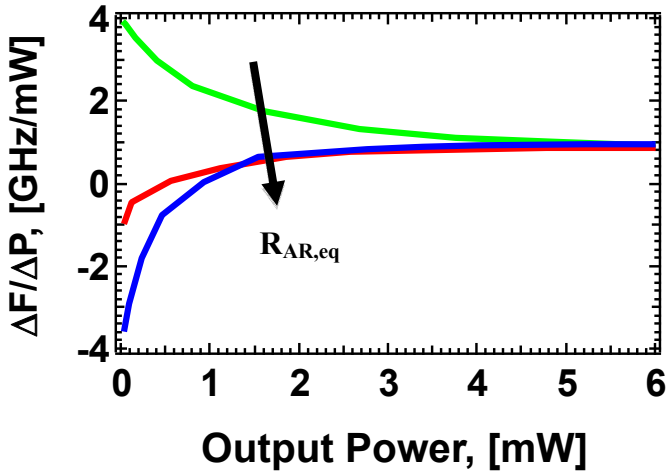

Fig. 9. Calculated adiabatic chirp as a function of the output power for various feedback conditions for κL=0.5 and L=350 μm

IV. CONCLUSIONS

The chirp induced by the optical modulation of a QW DFB diode laser is evaluated through the measure of the CPR. Optical feedback is found to suppress the thermal chirp, which is primarily attributed to a modification of the threshold voltage across the *pn* junction. On the other hand, experimental results have demonstrated that under the best optical feedback conditions the adiabatic CPR is significantly decreased from about 650 MHz/mW in the solitary case down to 65 MHz/mW. This last achievement is of first importance for improving the transmission capabilities in optical telecommunication systems. Such experimental results have been confirmed by numerical investigations based on the transfer matrix method. Simulations also have pointed out the possibility to optimize the adiabatic chirp by considering a judicious cavity design associated to a proper external control. Further studies will investigate the effects of the optical feedback on the chirp under large signal analysis as well as in quantum dot nanostructure based semiconductor lasers for which the SHB effects are expected to be larger [17].

REFERENCES

[1] Petermann, K., "Laser Diode Modulation and Noise", Kuwer Academic Publisher(1991).
[2] Coldren, L. A., and Corzine, S. W., "Diode Lasers and Photonic Integrated Circuits", Wiley(1995).
[3] Grillot, F., Thedrez, B., Py, J., Gauthier-Lafaye, O., Voiriot, V., and Lafragette, J. L., "2.5Gbit/s transmission characteristics of 1.3µm DFB lasers with external optical feedback," IEEE Photon. Technol. Lett., 14(1), 101-103(2002).
[4] Kane, D. M. and Shore, K. A., "Unlocking dynamical diversity", Wiley, 23-54(2005).
[5] Shunk, N. and Petermann, K., "Numerical analysis of the feedback regimes for a single-mode semiconductor laser with external feedback", IEEE J. Quantum Electron., 24(7), 1242-1247(1988).
[6] Henry, C. and Kazarinov, R. F., "Instabilities of semiconductor lasers due to optical feedback from distant reflectors", IEEE J. Quantum Electron., 22(2), 294-301(1986).
[7] Grillot, F., Thedrez, B., Mallecot, F., Chaumont, C., Hubert, S., Martineau, M.F., and Pinquier, A., "Analysis, Fabrication and Characterization of 1.5µm Selection-Free Tapered Stripe DFB Lasers," IEEE Photonics Technology Letters, 14(8), 1040-1042(2002).
[8] Provost, J. G., and Grillot, F., "Measuring the Chirp and the Linewidth Enhancement Factor of Optoelectronic Devices with a Mach-Zehnder Interferometer," IEEE Photonics Journal, 3(3), 476-488(2011).
[9] Shunk, N. and Petermann, K., "Numerical analysis of the feedback regimes for a single-mode semiconductor laser with external feedback", IEEE J. Quantum Electron., 24(7), 1242-1247(1988).
[10] Schimpe, R., Bowers, J. E., and Koch, T. L., "Characterization of frequency response of 1.5-µm InGaAsP DFB laser diode and InGaAs PIN photodiode by heterodyne measurement technique, " Electron. Lett., 22(9), 453–454(1986).
[11] Grillot, F., "On the Effects of an Antireflection Coating Impairment on the Sensitivity to Optical Feedback of AR/HR Semiconductor DFB Lasers", IEEE J. Quantum Electron., (45)6, 720-728(2009).
[12] Thedrez, B., Rainsant, J.M., Aberkane, N., Andre, B.; Bissessur, H., Provost, J. G., Fernier, B, "Power and facet phase dependence of chirp for index and gain-coupled DFB lasers," paper TuE41, Semiconductor Laser Conference, 175-176(1998).
[13] Mitsuhashi, Y., Shimada, J., Mitsutsuka, S., "Voltage change across the self-coupled semiconductor laser", IEEE J. Quantum Electron., 17(7), 1216-1225(1981).
[14] Bjork, K and Nilsson, O., "A new exact and efficient numerical matrix theory of complicated laser structures: properties of asymmetric phase-shifted DFB lasers", IEEE J. Lightwave Technol., 5(1), 140-146(1987).
[15] Orfanos, I and Sphicopoulos, T, "A tractable above-threshold model for the design of DFB and phase-shifted DFB lasers", IEEE Quantum electronics, 27(4), 946-956(1991).
[16] Grillot, F., Thedrez, B., Voiriot, V., and Lafragette, J. L., "Coherence collapse threshold of 1.3µm semiconductor DFB lasers", IEEE Photon. Technol. Lett., 15(1), 9-11(2003).
[17] Asryan, L. V., and Suris R. A., "Longitudinal spatial hole burning in a quantum-dot laser," IEEE J. Quantum Electron., 36(10), 1151– 1160(2000).

Acknowledgements: The authors are grateful to the MODULE project from the French national initiative ANR-VERSO program and SYSTEMATIC Paris-Region for financial support.